AGU PUBLICATIONS

Geophysical Research Letters

RESEARCH LETTER
10.1002/2013GL058680

Key Points:
- During a tsunami, currents are a primary cause of damage in ports and harbors
- Such currents have not been accurately described, thus underestimating hazards
- Products and guidance will be used to set national standards for harbors

Supporting Information:
- Readme
- Table S1 and Figures S1 and S2

Correspondence to:
P. J. Lynett,
plynett@usc.edu

Citation:
Lynett, P. J., J. Borrero, S. Son, R. Wilson, and K. Miller (2014), Assessment of the tsunami-induced current hazard, *Geophys. Res. Lett.*, *41*, 2048–2055, doi:10.1002/2013GL058680.

Received 18 NOV 2013
Accepted 30 JAN 2014
Accepted article online 5 FEB 2014
Published online 18 MAR 2014

Assessment of the tsunami-induced current hazard

Patrick J. Lynett[1], Jose Borrero[1,2], Sangyoung Son[1,3], Rick Wilson[4], and Kevin Miller[5]

[1]Department of Civil and Environmental Engineering, University of Southern California, Los Angeles, California, USA, [2]eCoast Marine Consulting and Research, Raglan, New Zealand, [3]Now at University of Ulsan, Ulsan, South Korea, [4]California Geological Survey, Sacramento, California, USA, [5]California Governor's Office of Emergency Services, Mather, California, USA

Abstract The occurrence of tsunami damage is not limited to events causing coastal inundation. Even without flooding, maritime assets are vulnerable to significant damage from strong currents and associated drag forces. While such impacts have been observed in the past, they have not been well studied in any context. Nearshore tsunami currents are governed by nonlinear and turbulent physics and often have large spatial and temporal variability making high-fidelity modeling particularly challenging. Furthermore, measured data for the validation of numerical simulations is limited, with few quality data sets appearing after recent tsunami events. In this paper, we present a systematic approach for the interpretation of measured tsunami-induced current impacts as well as a validation approach for simulation tools. The methods and results provided here lay the foundation for much needed efforts to assess tsunami hazards in ports and harbors.

1. Introduction

Recent transoceanic tsunami events have highlighted the vulnerability of maritime infrastructure to tsunami-induced currents. While tsunami currents are an obviously significant and damaging component of large-scale tsunami inundation from near-field sources, the potential for damage at maritime facilities due to currents induced by tsunami surges not causing inundation (and usually from far-field sources) is much less studied or understood. In recent years, the effects of tsunami currents in nearshore areas have been reported from many locations. This includes the observations of *Okal et al*. [2006a, 2006b, 2006c] who described three cases following the 2004 Indian Ocean tsunami where large ships broke free from mooring lines and drifted uncontrolled through their respective ports. One of the most remarkable observations was in the Port of Salalah, Oman, where 90 min after tsunami arrival, strong currents broke all of the mooring lines securing the 285 m freighter R/V *Maersk Mandraki* and pulled it away from the terminal. The ship was reportedly caught in a system of eddies and could not be brought under control even with the use of tugboats. Numerical hindcasts of the event suggest that tsunami currents in the vicinity of the vessel were approximately 8–10 knots (4–5 m/s) [*Lynett et al*., 2012]. The other two cases reported by Okal et al. in Madagascar and Reunion Island, were similar in that the strongest currents were observed well after tsunami arrival and no flooding of port facilities occurred.

Two years later in November 2006, Crescent City Harbor in California was affected by tsunami currents resulting from a *M* 8.3 earthquake in the Kuril Islands. Very strong currents were reported beginning with the initial waves and intensifying as the larger surges came through, resulting in severe damage to several docks, particularly those located nearest to the entrance of the inner harbor [*Dengler et al*., 2008]. In February 2010, ports in California were again affected by tsunami currents following the *M* ~8.8 Maule, Chile earthquake. Surges began affecting San Diego around midday on 27 February and steadily moved northward over the next several hours. Currents of up to 16 knots (8 m/s), visually estimated by eyewitnesses, caused damage to docks in San Diego, Catalina Island, Ventura, and Santa Cruz and affected passengers boarding a cruise ship in Los Angeles [*Wilson et al*., 2013].

The 2011 Tohoku tsunami was the most widely instrumented and recorded tsunami in history, and a handful of flow speed measurements are found in the literature [e.g., *Fritz et al*., 2012; *Hayashi and Koshimura*, 2013]. In the far field, every port, harbor, and maritime facility along the U.S. West Coast was adversely affected by surges and currents induced by the 2011 Tohoku tsunami [*Wilson et al*., 2012, 2013] with the strongest effects and most severe damage occurring in Crescent City and Santa Cruz. Tsunami surges produced very strong currents in Crescent City's inner harbor destroying docks and boats present at the time of the tsunami. The Tohoku tsunami also caused current related damage in New Zealand [*Borrero et al*., 2013] and the Galapagos Islands [*Lynett et al*., 2013] among other locations around the Pacific Rim.

Table 1. Damage Index and Corresponding Damage Type

Damage Index	Damage Type
0	no damage/impacts
1	small buoys moved
2	1–2 docks/small boats damaged and/or large buoys moved
3	Moderate dock/boat damage (<25% of docks/vessels damaged) and/or midsized vessels off moorings
4	Major dock/boat damage (<50% of docks/vessels damaged) and/or large vessels off moorings
5	Extreme/complete damage (>50% of docks/vessels damaged)

The events described above highlight the vulnerability of maritime facilities to tsunamis that do not cause inundation yet present potentially adverse conditions that may exist for many hours after tsunami arrival. While the phenomenon of dangerous, damaging currents has been observed repeatedly in the past, it has not been well studied in the context of hazard mitigation. This is due in large part to the fact that previous efforts have focused on the first-order issue of inundation. Additionally, it must be recognized that resolving tsunami velocities with numerical models is computationally intensive, requiring relatively fine computational mesh sizes resulting in numerical grid dimensions that are very large with extremely long run times, making them impractical for many modeling efforts. Furthermore, while there are several estimates of current speed based on eyewitness accounts, there is a paucity of quantitative instrumental or observed data on tsunami-induced current speeds making model calibration and validation difficult. Here we present a foundation for understanding current-based tsunami hazards in the coastal zone, demonstrating a validation and sensitivity analysis followed by application of numerical simulation tools for hazard mapping purposes.

2. Relating Current Speed to Damage

As a first step into the investigation of tsunami currents and maritime hazard, we compiled a database of tsunami current speed and associated damage. Recorded damage observations in ports and harbors are somewhat limited, with good data available only from events of the past decade. As such, this data set is dominated by observations gathered in California following the 2010 Chile and 2011 Tohoku tsunamis [*Wilson et al*., 2013] and augmented by additional observations found in *Lynett et al*. [2012, 2013] and *Borrero et al*. [2013] (Table S1, in the supporting information). Typically, damage observations are accompanied by eyewitness estimates of the local current speed; however, the fidelity of these estimates varies greatly, from a low confidence estimates taken from distances greater than 10 m from the water to those taken at or in the water by experienced boat captains. Furthermore, instrumental measurements of currents in the vicinity of damaged structures are rare, leaving select few data sets appropriate for model validation. However, with comparison to these measured field data sets in conjunction with experimental benchmarking, we are able to use modeling tools to realistically estimate currents in ports and harbors.

To connect current speed with damage state, we divide the damage state in to six indices, listed in Table 1. While the damage type, and thus the resulting index, is subjective, a review of the observed types of damage suggests that these categories provide a reasonably complete coverage of tsunami impacts in harbors. Based on this damage categorization, we plot current speed versus damage index, as shown in Figure 1. We note that this figure shows only instrumental data and numerical hindcasts and does not include eyewitness estimates since such observations generally report current speeds that are on average twice the numerical or instrumental values. This discrepancy is likely the result of a range of factors but mostly due to overestimation by eyewitnesses inexperienced in estimating current velocities. From the opposite standpoint, there may be a discrepancy due to the inability of numerical simulations to resolve the highly localized strong currents that eyewitnesses may focus on. However, this is a moot point in that current-based hazard maps will ultimately be based on simulated current speeds. Therefore, the correlation between simulated currents and damage states is important while correlation between simulated currents and eyewitness estimates is secondary.

Although damage in harbors might vary based on the age and location of docks and boats, some generalities about the relationship between tsunami currents and damage can be determined. As expected, Figure 1 shows a general trend of increasing damage with increasing current speed. In this data, there is a noticeable threshold for damage initiation at ~3 knots (1.5 m/s). When 3 knots is exceeded, the predicted damage state switches from no damage to minor-to-moderate damage. Thus, in the simulated data, 3 knots represents the

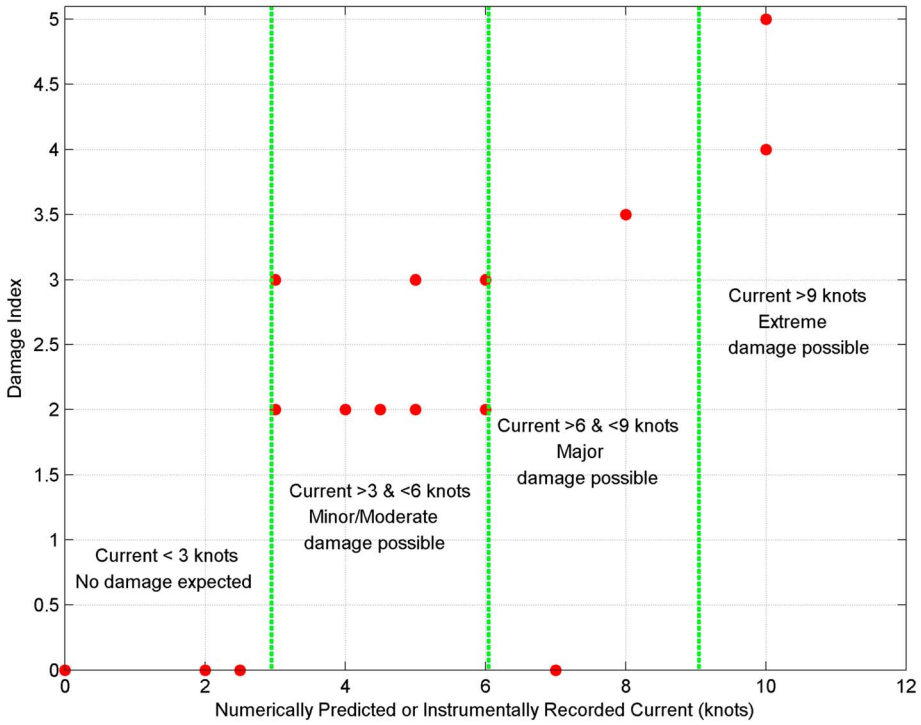

Figure 1. Scatter plot of observed damage indices and their corresponding tsunami-induced current.

first important current velocity threshold. We then argue that the second threshold is at 6 knots (3 m/s), where damage transitions from moderate to major. A third current speed threshold is less clear, but is logically around 9 knots (4.5 m/s), where damage levels move to the extreme damage category; additional damage observations with correlated current predictions are needed to better define this threshold. These three current divisions will be used to categorize potential damage levels in subsequent analysis of tsunami currents in ports and harbors.

3. Modeling Approach and Justification

For this study, we assessed modeled currents from a suite of model scenarios representing both near-and far-field tsunami sources relative to the northern California coast. Sources included historical events such as the 2010 and 2011 tsunamis originating from Chile and Japan as well as hypothetical tsunamis generated by large earthquakes along the Alaska-Aleutian Islands Subduction Zone and the Cascadia Subduction Zone. A majority of the hydrodynamic results presented here come from the application of the "Method of Splitting Tsunami" (MOST) numerical model [*Titov and González*, 1997]. The MOST model has been used extensively for tsunami hazard assessments in the United States and is currently in operational tsunami forecast use at the National Oceanic and Atmospheric Administration's (NOAA) Pacific Marine Environmental Laboratory. Variants of the MOST model have been in constant use for tsunami hazard assessments in California since the mid-1990s. Due to the extensive previous usage of MOST, and the fact that its background is generally well known, additional theoretical details of the model will not be provided here. For select cases, the MOST results are compared to numerical model results from COULWAVE, a high-order Boussinesq-type model developed over the past decade with the particular goal of understanding rotational flow in shallow water. Recent contributions to the model [e.g., *Kim et al.*, 2009; *Kim and Lynett*, 2011; *Son et al.*, 2011] allow for inclusion of the viscous effects of a bottom shear and associated rotationality directly in a Boussinesq-type derivation. While this leads to a far more complex set of model equations as compared to MOST, it includes the physics necessary to simulate boundary shear, and the complete coupling of these effects with a nonlinear, dispersive wave field. This model can also predict the friction-induced changes to the vertical profile of velocity under unsteady flow, and thereby can provide good estimates of internal kinematics.

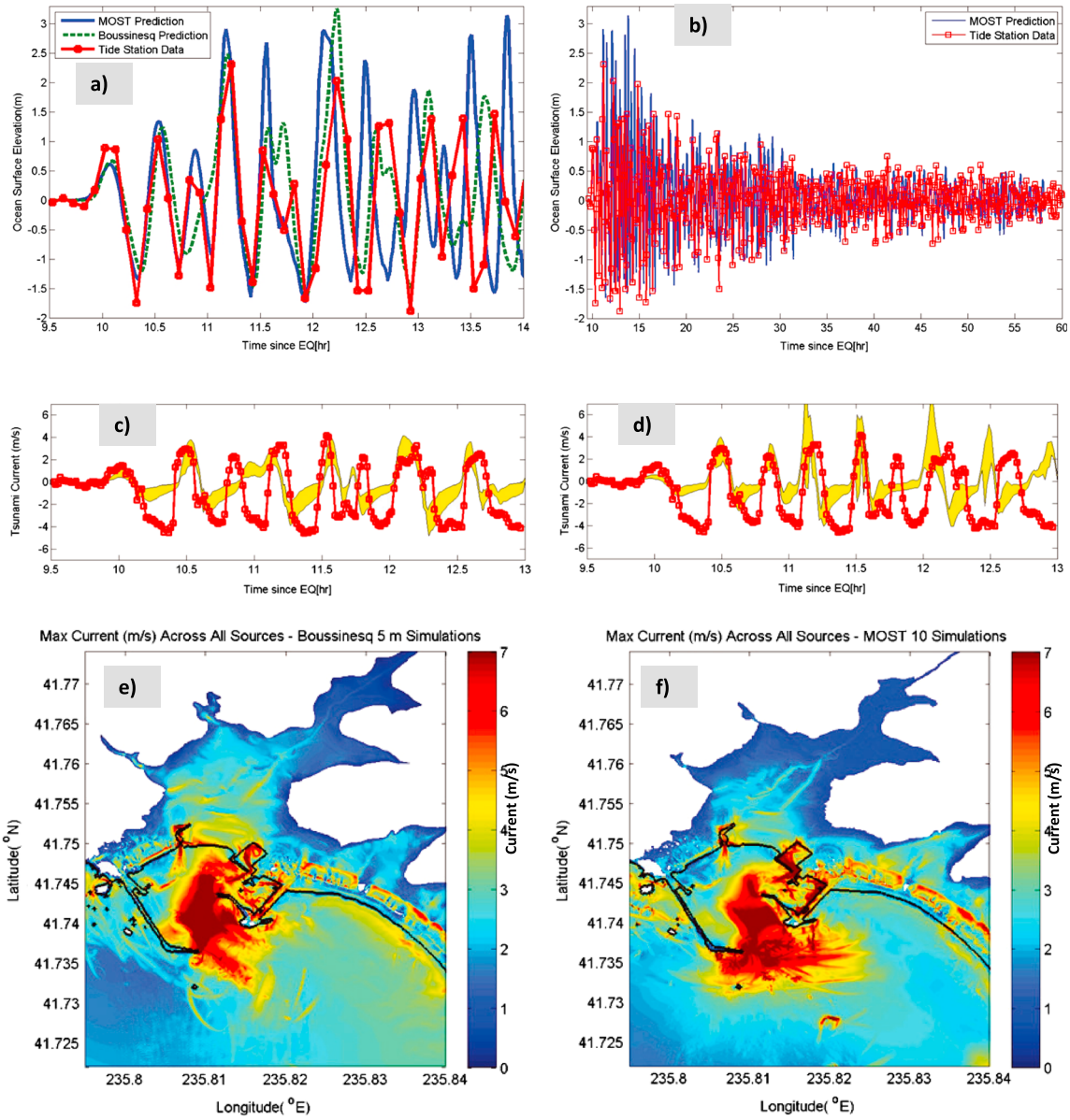

Figure 2. Validation and comparison of numerical simulation tools for water surface elevation and currents in Crescent City, CA; (a) comparison of MOST (blue solid), Boussinesq (green dashed), and tide station data (red solid + dots) for the 2011 Tohoku tsunami; (b) comparison of MOST (blue solid) and tide station data (red solid + dots) for 60 h post-EQ; (c) comparison of fluid speed (m/s) at inner boat basin entrance between Boussinesq (yellow) and digitized video data (red solid + dots); (d) comparison of fluid speed (m/s) at inner boat basin entrance between MOST (yellow) and digitized video data (red solid + dots); (e) maximum speed predicted by COULWAVE across a range of different tsunami sources; and (f) maximum speed predicted by MOST across a range of different tsunami sources.

In this study, MOST is used to propagate tsunami waves from source to the nearshore region, using a system of nested grids. The outermost grid at 4 arc min resolution covers the entire Pacific basin. Three additional grids of increasingly finer resolution were derived from data provided by NOAA's National Geophysical Data Center specifically for tsunami forecasting and modeling efforts. The innermost nearshore grid with the highest resolution is used with both the MOST (10 m resolution) and COULWAVE (5 m resolution) models, with boundary input from the previous MOST nested layer. Figures 2a–2d compare model output to measured values of water level and current speeds in Crescent City during the 2011 Tohoku tsunami. Water levels were recorded on the local tide gauge while current speeds were estimated through visual particle tracking using video footage recorded on a security camera with a clear view of the inner harbor entrance channel [*Admire et al.*, 2011, 2013].

From Figure 2a, we can see that both the 5 m resolution Boussinesq and 10 m resolution MOST results provide a reasonably accurate prediction of the sea surface elevation. Both the phase (arrival time of crests) and heights of the individual waves are well captured. Note that in order to match the arrival time of the measured leading wave, the numerical time series are shifted 10 min (0.17 h) earlier. This shift is explained through lack of water compressibility and neglect of the effects of Earth's elasticity [*Tsai et al.*, 2013] in the MOST propagation model, resulting in waves that arrive slightly earlier than measured. After approximately 2 h, the phase of the 10 m MOST results diverges from the data while the Boussinesq stays in phase for another two wave cycles. By 3.5 h into the event, however, both models exhibit phase errors, and thus after this time can only be statistically compared to measured data. The cause of these phase errors can be attributed to a range of factors such as: lack of dispersion in the transoceanic propagation grids, lack of dispersion and turbulence effects in the 10 m harbor grid in the MOST model, numerical dispersion and dissipation errors, poor or missing resolution of features in the bathymetric data, lack of inclusion of tides, and poor or missing resolution of reflected energy from neighboring and distant shorelines. To evaluate the behavior of the MOST model for very long duration simulations, we compare model output to ~50 h of tide gauge data (Figure 2b). While there is little phase correlation between the model and measured data, the envelope of wave height decay is accurately captured. From this comparison, it can be stated with some foundation that the MOST model is able to provide a realistic estimate of the wave height envelope for very long duration simulations. Confirming validity of ability to model duration has important real-world safety applications for mariners and port authorities.

While tsunami prediction models are regularly compared with sea surface elevation data, validation against measured current data is less common. The primary reasons for this missing class of comparison is the lack of current data and a previous focus on the leading order prediction of inundation and runup for evacuation planning. Furthermore, it is well known that when examining wave-driven free surface flows, small errors in sea surface phase and amplitude lead to large errors in fluid speed; velocity comparisons are considerably more challenging than sea surface comparisons. With this in mind, model-data comparisons for speed at the entrance to the small boat basin are given in Figures 2c and 2d for MOST and COULWAVE, respectively. Numerical results extracted from model grid nodes within 10 m of the measurement location are used to generate the yellow envelope of predicted current speeds.

To match the arrival time of the numerically predicted wave with the measured wave, the same time shift applied to match the first wave in the tidal station record is applied here. A different time shift was not, and should not, be used here to provide a good phase match with the leading velocity peak; only a single time shift can be used for all data comparisons. The shape and peaks of the speed record are reasonably well captured by the models. While the COULWAVE results are somewhat better in terms of capturing the data maxima and minima, both models include these maxima and minima within the yellow envelope. There is also larger spatial variation in the MOST results as compared to COULWAVE, as can be inferred from the vertical width of the yellow envelope.

Finally, in Figures 2e and 2f we compare the maximum predicted current speeds across all tested tsunami sources from the 5 m grid COULWAVE simulations and the 10 m MOST simulations. Spatially, the current speed patterns show a general similarity, but there are significant localized differences. Near the boundaries of the small boat basin and near coastal structures in general, the MOST model provides current estimates that are greater than COULWAVE. This difference is attributed to how MOST handles water overtopping structures. As this phenomenon is complex, it is not straightforward to identify which model is "correct". The zonation derived from the model results matches well with observations of currents and damage in Crescent City harbor [*Wilson et al.*, 2012].

4. Hazard Assessment in Ports and Harbors

Examples of the types of simulation-based information that should be useful for hazard assessment in coastal areas are shown in Figure 3. In Figure 3a, we plot maximum current speed in Crescent City predicted from the 2011 Tohoku source with solid colors corresponding to the damage thresholds discussed above, i.e., less than 3 knots, 3 to 6 knots, 6 to 9 knots, or 9 knots and above. We see that the zonation matches well with observations of currents and damage in Crescent City Harbor (lower left inset, Figure 3a). Widespread areas of extreme and major damage zones are found in the small boat basin, where pilings, docks, and vessels were heavily damaged or destroyed.

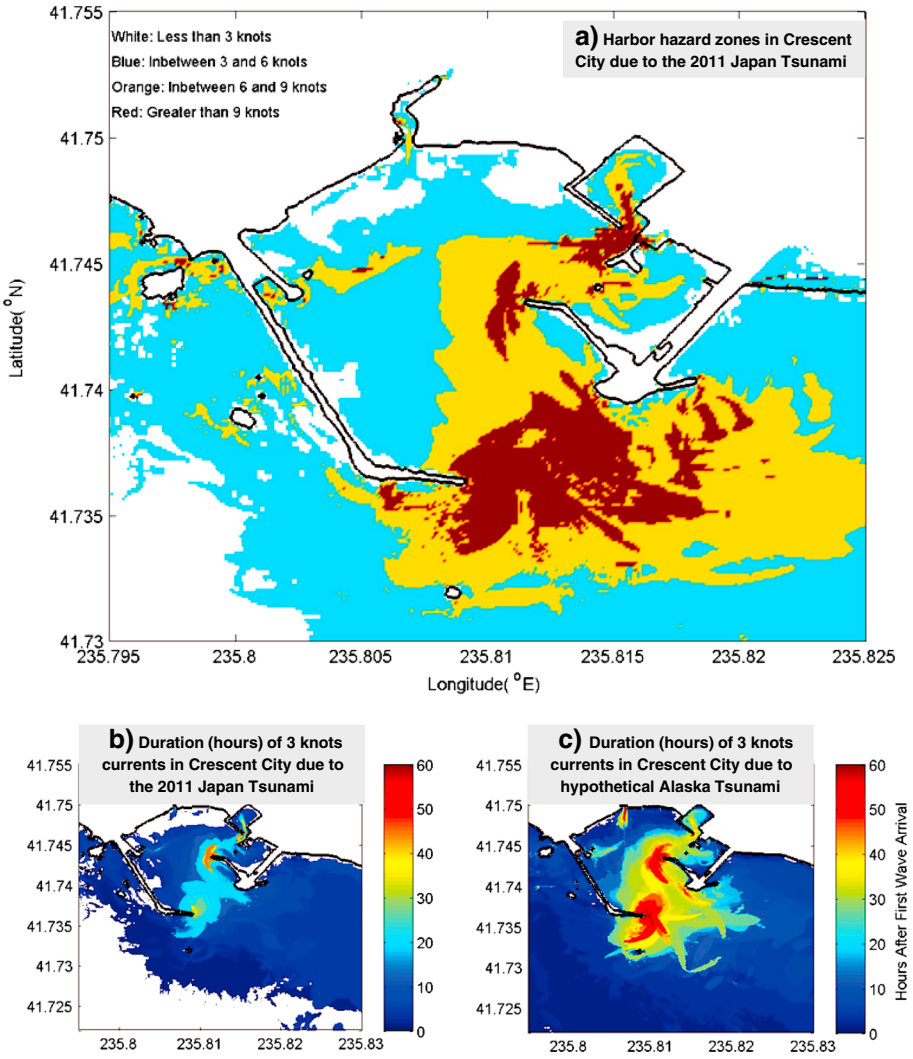

Figure 3. Example uses of the simulation output for hazard assessment. (a) Current speed hazard zones for 3/6/9 knot zonation. (b and c) Time-threshold maps are given for two different sources.

To determine the duration of damaging currents, "time-threshold" maps are generated. For a specified current, these maps will show the time duration during which the current is exceeded based on numerical modeling results run for a 60 h tsunami scenario. For example, a 6 knot time-threshold map which shows for a particular location a value of 3.4 h indicates that at that location, flow speeds of 6 knots are not exceeded after 3.4 h of waves. This metric allows for the estimation of how long damaging currents will be active, which could be different depending on the type of maritime assets at stake.

Figures 3b and 3c provide time-threshold maps for a single current speed (3 knots) for two different tsunami sources: the 2011 Tohoku source and a hypothetical M_w ~9.2 earthquake along the Eastern Aleutian Subduction Zone. The simulations predict that for the Tohoku event 3 knots currents should persist for up to 40 h near structures and for 20 h in the main harbor entrance channel, while for the Aleutian event, these values are 60+ h and 45 h, respectively. While this type of information should be very useful for harbor personnel to estimate the duration of potential impacts, the estimates will be highly source dependent.

5. Offshore Evacuation Depths for Vessels

In the event of a distant tsunami, wherein there is sufficient time to safely evacuate vessels from a harbor, an evacuation area can be provided for guidance. As most captains will be familiar with following fathom lines,

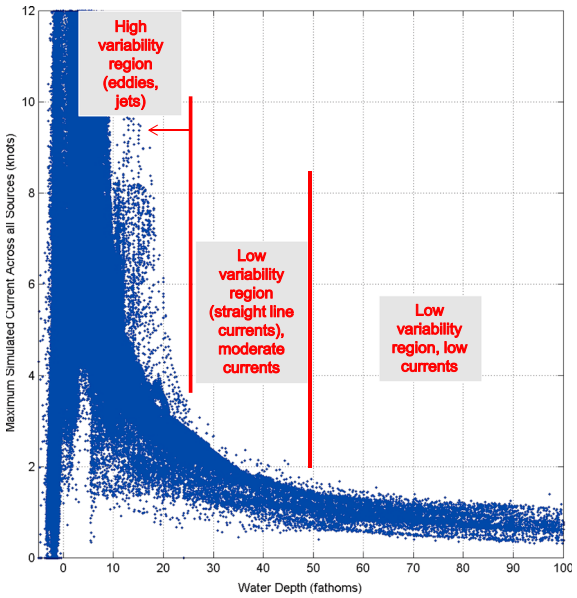

1 fathom = 1.8 meters = 6 feet

Figure 4. Scatter plot of maximum simulated current speed as a function of water depth for all sources, all grid resolutions, and all models.

we aim to specify a "safe depth," where hazardous conditions are not expected. There are a number of conditions which should be met for a depth to be given as "safe," such as no chance of vessel grounding, negligible wave steepness, and readily navigable currents. From our analysis, the condition of navigable currents is the controlling factor, requiring a depth where grounding and steepness are not significant concerns. From observations of tsunami-induced coastal currents in previous events, the challenges to coastal navigation are due to both strong currents and rapidly changing currents, in both time and space.

Taking the model output data, a scatter plot of maximum current and depth pairs is generated, as shown in Figure 4 for nearshore and offshore areas of Northern California. This information can be used to determine the mean or maximum expected current for a given water depth. It is found that maximum tsunami currents of less than 1 knot (0.5 m/s) are expected at a depth of 100 fathoms (~180 m). Large variations in the possible maximum current exist to a depth of approximately 25 fathoms (~45 m), indicating that this is the greatest depth that large eddies or jets might extend to. Depths greater than 30 fathoms (~55 m) will in general be safe, particularly for dispersed or larger vessels. This number may become a valuable, consistent future policy recommendation for vessel evacuation along California's coast.

6. Conclusions and Future Work

This study presents a detailed assessment of tsunami-induced current speeds in ports and harbors. Our model results suggest that while not as accurate as the higher-order COULWAVE model on a 5 m grid, the MOST tsunami model using a 10 m grid satisfactorily reproduces measured tsunami-induced current speeds. The trade off in accuracy is, however, compensated by the tendency for the MOST results to be conservative in terms of hazard assessment and by the fact that MOST is much less computationally demanding.

Model results from a range of scenarios can then be combined with information about tsunami amplitudes, currents, and damage from recent events (i.e., 2006 Kuril Islands, 2009 Samoa, 2010 Chile, 2011 Tohoku, and 2012 British Columbia) to develop an emergency response "decision tree" which will allow forecast information from future tsunamis to be quickly and easily compared to particular real or modeled scenarios and determine an appropriate course of action. The results of this type of analysis are being used to develop a suite of map products and policy guidance documents for maritime communities to know if, when, and where strong tsunami currents will occur and whether vessels should be relocated within or outside of a harbor during and in advance of a tsunami. This maritime mapping plan and guidance will likely also form the basis for national standards through the U.S. National Tsunami Hazard Mitigation Program [*Wilson and Eble*, 2013].

Acknowledgments

The authors thank Stefano Lorito and an anonymous reviewer for their constructive comments on this paper. Research presented in this paper was supported by grants through the California Geological Survey, the California Governor's Office of Emergency Services, and the National Science Foundation award #1135026.

The Editor thanks Stefano Lorito and an anonymous reviewer for their assistance in evaluating this paper.

References

Admire, A. R., L. A. Dengler, G. B. Crawford, B. U. Uslu, J. Montoya, and R. I. Wilson (2011), Observed and modeled tsunami current velocities on California's north coast: 2011 Fall Meeting, AGU, San Francisco, Calif., abstract NH14A-03.

Admire, A. R., L. A. Dengler, G. B. Crawford, B. U. Uslu, J. Borrero, S. D. Greer, and R. I. Wilson (2013), Observed and modeled currents from the Tohoku-oki, Japan and other recent tsunamis in northern California, *Pure Appl. Geophys.*, doi:10.1007/s00024-014-0797-8.

Borrero, J., R. Bell, C. Csato, W. DeLange, D. Greer, D. Goring, V. Pickett, and W. Power (2013), Observations, effects and real time assessment of the March 11, 2011 Tohoku-oki Tsunami in New Zealand, *Pure Appl. Geophys.*, *170*, 1229–1248, doi:10.1007/s00024-012-0492-6.

Dengler, L. A., B. Uslu, A. Barberopoulou, J. C. Borrero, and C. Synolakis (2008), The vulnerability of Crescent City, California, to tsunamis generated by earthquakes in the Kuril Islands region of the northwestern Pacific, *Seismol. Res. Lett.*, *79*(5), 608–619.

Fritz, H., D. A. Phillips, A. Okayasu, T. Shimozono, H. Liu, F. Mohammed, V. Skanavis, C. E. Synolakis, and T. Takahashi (2012), The 2011 Japan tsunami current velocity measurements from survivor videos at Kesennuma Bay using LiDAR, *Geophys. Res. Lett.*, *39*, L00G23, doi:10.1029/2011GL050686.

Hayashi, S., and S. Koshimura (2013), The 2011 Tohoku Tsunami flow velocity estimation by the aerial video analysis and numerical modeling, *J. Disaster Res.*, *8*(4), 561–572.

Kim, D.-H., P. Lynett, and S. Socolofsky (2009), A depth-integrated model for weakly dispersive, turbulent, and rotational fluid flows, *Ocean Modell.*, *27*(3-4), 198–214.

Kim, D.-H., and P. Lynett (2011), Turbulent mixing and scalar transport in shallow and wavy flows, *Phys. Fluids*, *23*(1), 016603, doi:10.1063/1.3531716.

Lynett, P., J. Borrero, R. Weiss, S. Son, D. Greer, and W. Renteria (2012), Observations and modeling of tsunami-induced currents in ports and harbors, *Earth Planet. Sci. Lett.*, *327–328*, 68–74.

Lynett, P., R. Weiss, W. Renteria, G. De La Torre Morales, S. Son, M. Arcos, and B. MacInnes (2013), Coastal impacts of the March 11th Tohoku, Japan Tsunami in the Galapagos Islands, *Pure Appl. Geophys.*, *170*, 1189–1206, doi:10.1007/s00024-012-0568-3.

Okal, E. A., H. M. Fritz, R. Raveloson, G. Joelson, P. Pancoskova, and G. Rambolamanana (2006a), Madagascar field survey after the December 2004 Indian Ocean tsunami, *Earthquake Spectra*, *22*, S263–S283.

Okal, E. A., H. M. Fritz, P. E. Raad, C. E. Synolakis, Y. Al-Shijbi, and M. Al-Saifi (2006b), Oman field survey after the December 2004 Indian Ocean tsunami, *Earthquake Spectra*, *22*, S203–S218.

Okal, E. A., A. Sladen, and E. A.-S. Okal (2006c), Rodrigues, Mauritius and Réunion Islands, field survey after the December 2004 Indian Ocean tsunami, *Earthquake Spectra*, *22*, S241–S261.

Son, S., P. Lynett, and D.-H. Kim (2011), Nested and multi-physics modeling of tsunami evolution from generation to inundation, *Ocean Modell.*, *38*(1–2), 96–113, doi:10.1016/j.ocemod.2011.02.007.

Titov, V. V., and F. I. González (1997), Implementation and testing of the Method of Splitting Tsunami (MOST) model NOAA Technical Memorandum ERL PMEL-112, 11 pp.

Tsai, V., J.-P. Ampuero, H. Kanamori, and D. Stevenson (2013), Estimating the effect of Earth elasticity and variable water density on tsunami speeds, *Geophys. Res. Lett.*, *40*, 492–496, doi:10.1002/grl.50147.

Wilson, R., and M. Eble (2013), New activities of the U.S. National Tsunami Hazard Mitigation Program, Mapping and Modeling Subcommittee, presented at 2013 Fall Meeting, AGU, San Francisco, Calif, abstract NH54A-05.

Wilson, R., C. Davenport, and B. Jaffe (2012), Sediment scour and deposition within harbors in California (USA), caused by the March 11, 2011 Tohoku-oki Tsunami, *Sediment. Geol.*, *282*, 228–240, doi:10.1016/j.sedgeo.2012.06.001.

Wilson, R. I., et al. (2013), Observations and impacts from the 2010 Chilean and 2011 Japanese tsunami in California (USA), *Pure Appl. Geophys.*, *170*, 1127–1147, doi:10.1007/s00024-012-0527-z.